

## A distributed small signal equivalent circuit modeling method for InP HEMT

QI Jun-Jun<sup>1</sup>, LYU Hong-Liang<sup>1\*</sup>, CHENG Lin<sup>1</sup>, ZHANG Yu-Ming<sup>1</sup>, ZHANG Yi-Men<sup>1</sup>, ZHAO Feng-Guo<sup>2</sup>,  
DUAN Lan-Yan<sup>2</sup>

(1. School of Microelectronics, Xidian University, Key Laboratory of Wide Band-Gap  
Semiconductor Materials and Devices, Xi'an 710071, China;  
2. ZTE Corporation, Shenzhen 518057, China)

**Abstract:** A distributed small signal equivalent circuit modeling method for InP high electron mobility transistor (HEMT) was presented. The distributed capacitance effect was considered in the adopted model, which is characterized by adding three distributed capacitances. For accurate modeling, the parasitic inductances are extracted first, considering the errors introduced by the parasitic inductances when extracting the parasitic capacitance first. The validity of the proposed small signal modeling method has been verified with excellent agreement between the measured and modeled results up to 50 GHz for InP HEMT. In addition, the S-parameters' modeling error is less than 4% in 2 ~ 50 GHz, which also proves the high accuracy of the proposed modeling method.

**Key words:** distributed model, small signal model, model parameters, extraction methods, high electron mobility transistor (HEMT)

**PACS:** 85. 30. De, 85. 30. Tv

## 一种 InP HEMT 分布小信号模型建模方法

戚军军<sup>1</sup>, 吕红亮<sup>1\*</sup>, 程林<sup>1</sup>, 张玉明<sup>1</sup>, 张义门<sup>1</sup>, 赵锋国<sup>2</sup>, 段兰燕<sup>2</sup>

(1. 西安电子科技大学微电子学院 宽禁带半导体技术国防重点学科实验室, 陕西 西安 710071;  
2. 中兴通讯股份有限公司, 广东 深圳 518057)

**摘要:**提出了一种用于 InP 高电子迁移率晶体管 (high electron mobility transistor, HEMT) 的分布式小信号等效电路建模方法。在采用的模型中考虑了分布电容效应, 通过加入三个分布电容来表征。为了精确建模, 在提取寄生电容时考虑到寄生电感引入的误差, 首先提取了寄生电感。在达到 50 GHz 的 InP HEMT 中, 小信号建模方法的有效性得到了验证。此外, 在 2 ~ 50 GHz 频率范围内, S 参数建模误差小于 4%, 这也证明了所提出建模方法的高建模精度。

**关键词:** 分布式模型; 小信号模型; 模型参数; 提取方法; 高电子迁移率晶体管

中图分类号: TN386 文献标识码: A

### Introduction

With the continuous development of RF wireless communication system, the demand for high-performance and low-cost RF solutions is increasing<sup>[1]</sup>. Compare to traditional Si and Ge-based CMOS devices, InP HEMT transistors have better frequency response characteristics, power density and breakdown voltage, which makes InP HEMT transistors become an excellent candi-

date for many monolithic microwave integrated circuits (MMICs) working at GHz frequency range<sup>[2]</sup>. As an important link between transistors and circuits, a large signal model which can accurately simulate dc, S-parameters and large signal characteristics determines the accuracy of circuits. Meanwhile, small signal model is the approximation of the large signal model at a single bias point<sup>[3]</sup>. Therefore, the accuracy of the large signal model depends mostly on the small signal equivalent circuit

**Received date:** 2021- 05- 24, **revised date:** 2022- 01- 10

**收稿日期:** 2021- 05- 24, **修回日期:** 2022- 01- 10

**Foundation items:** Supported by the Project InP High Electron Mobility Transistor Noise Model Research and Technical Support in Cooperation with ZTE and the Key Research and Development Program of Shaanxi (2021GY-010)

**Biography:** QI Jun-Jun (1996- ), female, Henan, China, PhD. Research area involves RF microwave small signal model parameter extraction.  
E-mail: 193063040@qq. com

\* **Corresponding author:** E-mail: hllv@mail. xidian. edu. cn

model which can reflect the physical and electrical properties of the device [4].

In the past decades, various extraction techniques, including numerical optimization method [5] and direct extraction method [6-7] have been developed. The numerical optimization method uses the numerical method to find the optimal parameter value. Although it is very accurate, it depends largely on the initial value of the parameter and may not converge. The direct extraction method uses the analytical equations to obtain the expression of each parameter without optimization, but it is difficult to be applied to small signal model with complex topology.

In order to solve these problems, the method combining numerical optimization and direct extraction method is used to extract the equivalent circuit parameters. This method takes the parameter value obtained by the direct extraction method as the initial value of the optimization method, which not only maintains the accuracy of the optimization method, but also avoids the convergence problem.

## 1 A distributed small signal equivalent circuit model

A distributed small signal equivalent circuit model shown in Fig. 1 is used for  $4 \times 75 \mu\text{m}$  gate width,  $0.15 \mu\text{m}$  gate length of InP HEMT device. The 19-element model includes 12 bias-independent extrinsic parameters and 7 bias-dependent intrinsic parameters. Bias independent extrinsic elements consist of  $C_{pg}$ ,  $C_{pd}$ ,  $C_{pgd}$  (pad parasitic capacitances),  $L_g$ ,  $L_d$ ,  $L_s$  (pad parasitic inductances),  $R_g$ ,  $R_d$ , and  $R_s$  (extrinsic resistances of gate, drain, and source, respectively). In addition, the distributed capacitance effect of the InP HEMT becomes more and more significant as the frequency gets higher [8]. In this model,  $C_{dg}$ ,  $C_{dd}$  and  $C_{dgd}$  are used to describe the distributed capacitance effect between the gate fingers, while  $C_{pg}$ ,  $C_{pd}$  and  $C_{pgd}$  are used to characterize the parasitic capacitance between PAD and ground. Bias dependent intrinsic elements mainly include  $R_{is}$  (channel resistance),  $G_{ds}$  (drain conductance),  $g_m e^{-j\omega\tau}$  (transconductance),  $\tau$  (time delay),  $C_{gs}$ ,  $C_{gd}$ , and  $C_{ds}$  (gate to source, gate to drain and drain to source capacitances, respectively).

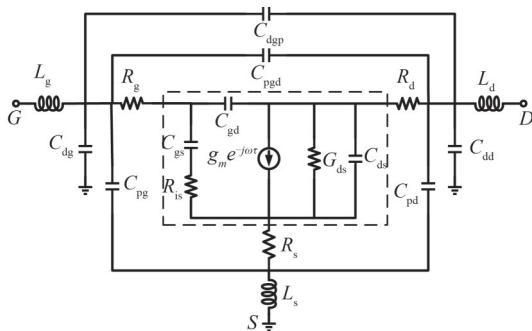


Fig. 1 Distributed small signal equivalent circuit model for InP HEMT

图1 InP HEMT 分布式小信号等效电路模型

## 2 Extrinsic model parameters extraction and verification

### 2.1 Parasitic inductances

The key of the small signal extrinsic parameter's extraction method is to simplify the equivalent circuit at a specific bias point in Fig. 1. Under cold pinch-off condition ( $V_{ds}=0$ ,  $V_{gs}<-V_{th}$ ), the drain source current source and output conductance are negligible, so the depletion region can be characterized by three capacitors  $C_{ig}$ ,  $C_{id}$  and  $C_{igd}$ , as shown in Fig. 2. Usually, the parasitic capacitances are extracted first, which cannot eliminate the effect of parasitic inductances. Consequently, the parasitic inductances  $L_g$ ,  $L_d$  and  $L_s$  must be de-embedded before extracting the parasitic capacitances, which is also the difference between the method in this paper and Gao's method [9].

Since parasitic resistances and inductances are sensitive at low frequencies, it is necessary to extract parasitic inductances at high frequencies ( $>25 \text{ GHz}$ ). In addition, the parasitic resistances don't affect the imaginary value of the Y parameters, so they can be excluded when extracting the parasitic inductances.

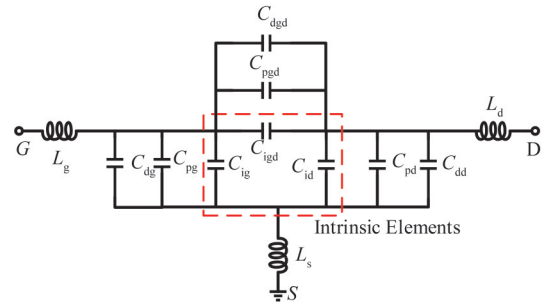


Fig. 2 Simplified Circuit for parasitic inductances extraction  
图2 提取寄生电感时的简化电路

The Z-parameters of the simplified circuit in Fig. 2 can be expressed as:

$$Z_{11} = j\omega(L_g + L_s) + \frac{C_{id} + C_{igd} + C_{xd} + C_{xgd}}{j\omega M}, \quad (1)$$

$$Z_{12} = Z_{21} = j\omega L_s + \frac{C_{igd} + C_{xgd}}{j\omega M}, \quad (2)$$

$$Z_{22} = j\omega(L_d + L_s) + \frac{C_{ig} + C_{igd} + C_{xg} + C_{xpg}}{j\omega M}, \quad (3)$$

where

$$C_{xg} = C_{pg} + C_{dg}, \quad (4)$$

$$C_{xd} = C_{pd} + C_{dd}, \quad (5)$$

$$C_{xpg} = C_{pgd} + C_{dgd}, \quad (6)$$

$$M = (C_{xg} + C_{ig} + C_{xgd} + C_{igd})(C_{xd} + C_{id} + C_{xgd} + C_{igd}) - (C_{xgd} + C_{igd})^2. \quad (7)$$

Multiplying the Z-parameters by  $\omega$  and the taking the imaginary parts gives:

$$\text{Im}(\omega Z_{11}) = \omega^2(L_g + L_s) - \frac{C_{id} + C_{igd} + C_{xd} + C_{xgd}}{M}, \quad (8)$$

$$\text{Im}(\omega Z_{12}) = \text{Im}(\omega Z_{21}) = \omega^2 L_s - \frac{C_{\text{igd}} + C_{\text{xgd}}}{M}, \quad (9)$$

$$\text{Im}(\omega Z_{22}) = \omega^2(L_d + L_s) - \frac{C_{\text{ig}} + C_{\text{igd}} + C_{\text{xg}} + C_{\text{xgd}}}{M}. \quad (10)$$

Consequently, the values of  $L_g$ ,  $L_d$  and  $L_s$  can be extracted from the slope of  $\text{Im}(Z_{ij})$  verse  $\omega^2$  as shown in Fig. 3.

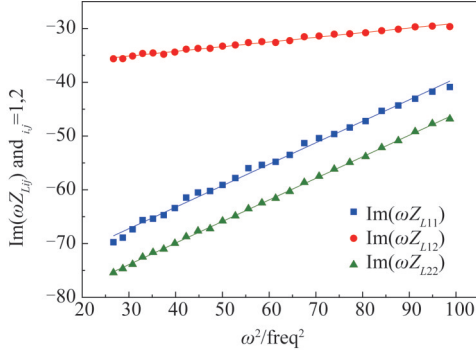


Fig. 3 Parasitic inductances extraction form the intercept of  $\text{Im}(Z_{ij})$  verse  $\omega^2$   
图3 从  $\text{Im}(Z_{ij})$  随  $\omega^2$  变化的截距中提取寄生电感

## 2.2 Parasitic capacitances

After de-embedding the parasitic inductances, parasitic capacitances  $C_{\text{pg}}$ ,  $C_{\text{pd}}$ ,  $C_{\text{pgd}}$  and distributed capacitances  $C_{\text{dg}}$ ,  $C_{\text{dd}}$  and  $C_{\text{dgd}}$  can be determined using device gate width scaling method [2].

Y-parameters of the simplified circuit shown in Fig. 2 can be written as:

$$\text{Im}(Y_{11})/\omega = C_{\text{xg}} + C_{\text{ig}} + C_{\text{igd}} + C_{\text{xgd}}, \quad (11)$$

$$\text{Im}(Y_{22})/\omega = C_{\text{xd}} + C_{\text{id}} + C_{\text{igd}} + C_{\text{xgd}}, \quad (12)$$

$$-\text{Im}(Y_{12})/\omega = C_{\text{igd}} + C_{\text{xgd}}. \quad (13)$$

The intrinsic capacitances  $C_{\text{ig}}$ ,  $C_{\text{id}}$  and  $C_{\text{igd}}$  are directly proportional to the gate-finger width, and the relationship between them can be described as:

$$C_{\text{ig}}(W) = C_{\text{ig0}}W, \quad (14)$$

$$C_{\text{id}}(W) = C_{\text{id0}}W, \quad (15)$$

$$C_{\text{igd}}(W) = C_{\text{igd0}}W. \quad (16)$$

By substituting Eqs. 14-16 into Eqs. 11-13, the total capacitances of gate source, gate drain and drain source branch can be obtained.

$$C_{\text{xg}} = \frac{\text{Im}(Y_{11})}{\omega} \Bigg|_{W \rightarrow 0} - C_{\text{xgd}}, \quad (17)$$

$$C_{\text{xd}} = \frac{\text{Im}(Y_{22})}{\omega} \Bigg|_{W \rightarrow 0} - C_{\text{xgd}}, \quad (18)$$

$$C_{\text{xgd}} = -\frac{\text{Im}(Y_{12})}{\omega} \Bigg|_{W \rightarrow 0}. \quad (19)$$

The capacitance  $C_{\text{xg}}$ ,  $C_{\text{xd}}$  and  $C_{\text{xgd}}$  can be calculated from Eqs. 17-19 with the Y-parameters measurements of

$4 \times 25 \mu\text{m}$ ,  $4 \times 50 \mu\text{m}$ ,  $4 \times 75 \mu\text{m}$ ,  $4 \times 100 \mu\text{m}$  and  $4 \times 150 \mu\text{m}$  InP HEMT. As shown in Fig. 4, the intercepts of  $\text{Im}(Y_{ij})/\omega$  ( $i, j=1, 2$ ) are the extracted values of  $C_{\text{xg}}$ ,  $C_{\text{xd}}$  and  $C_{\text{xgd}}$ .

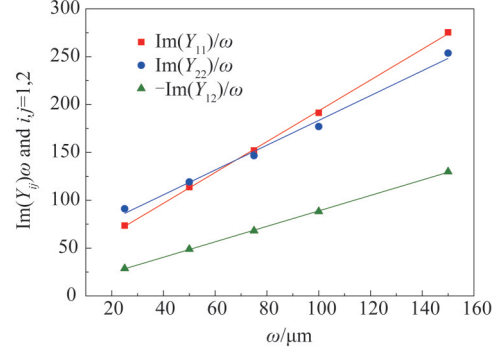


Fig. 4 Extrinsic capacitances extraction form the intercept of  $\text{Im}(Y_{ij})$  verse  $\omega$   
图4 从  $\text{Im}(Y_{ij})$  随  $\omega$  变化的截距中提取寄生电容

The next step is how to search for the optimal parasitic and distributed capacitances, which can ultimately minimize the error between the measured and simulated results. Before optimizing the extrinsic capacitances, the intrinsic capacitances  $C_{\text{ig}}$ ,  $C_{\text{id}}$  and  $C_{\text{igd}}$  can be determined using Eqs. 11~13:  $C_{\text{ig}}=70$  fF,  $C_{\text{id}}=52.9$  fF,  $C_{\text{igd}}=72$  fF. Unlike the small signal model of GaN HEMT in Ref. [10], the assumption of  $C_{\text{ig}} = C_{\text{igd}}$  cannot be used in the optimization process.

During optimization,  $C_{\text{dg}}$  is scanned from 0 to  $C_{\text{xg}}$ ,  $C_{\text{dd}}$  is scanned from 0 to  $C_{\text{xd}}$ , and  $C_{\text{dgd}}$  is scanned from 0 to  $C_{\text{xgd}}$ . In order to reduce the optimization difficulty, some specific extrinsic capacitance relations must be assumed [11]:

$$C_{\text{pg}} \approx C_{\text{pd}}, \quad C_{\text{dg}} \approx C_{\text{dd}}. \quad (20)$$

When the error between the measured and simulated results reaches a minimum, the values of parasitic and distributed capacitances can be determined.

## 2.3 Parasitic resistances

Figure 5 is the small signal circuit under  $V_{\text{gs}} > V_{\text{th}}$  and  $V_{\text{ds}}=0$ , the depletion region can be represented by channel distribution resistance  $R_c$  and gate differential resistance  $R_j$ .

The Z-parameters of the circuit as shown in Fig. 5 can be written as:

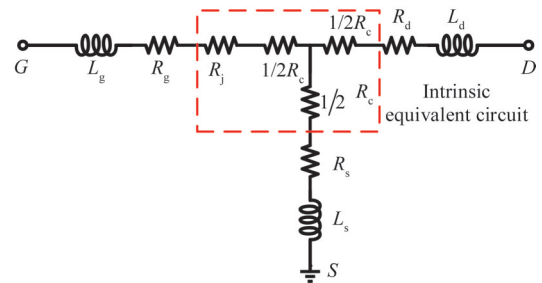


Fig. 5 Simplified Circuit for parasitic resistances extraction  
图5 提取寄生电阻时的简化电路

$$Z_{11} = R_s + R_g + R_j + j\omega(L_s + L_g) \quad , \quad (21)$$

$$Z_{12} = Z_{21} = R_s + 1/2R_j + j\omega L_s \quad , \quad (22)$$

$$Z_{22} = R_s + R_d + R_c + j\omega(L_s + L_d) \quad , \quad (23)$$

where  $R_j = nKT/qI_g$ ,  $I_g$  is the gate leakage current,  $n$  is the ideal factor of the schottky diode,  $k$  is the boltzmann constant,  $T$  is the kelvin temperature<sup>[11]</sup>. To extract parasitic resistances, the impact of  $R_j$  and  $R_c$  must be eliminated. Channel distribution resistance  $R_c$  is proportional to  $1/(V_{gs} - V_{th})$ <sup>[12]</sup>, the Eqs. 22-23 can be expressed as:

$$\text{Re}(Z_{22}) \Big|_{1/(V_{gs} - V_{th})=0} = R_s + R_d \quad , \quad (24)$$

$$\text{Re}(Z_{12}) \Big|_{1/(V_{gs} - V_{th})=0} = R_s \quad . \quad (25)$$

Therefore, it is necessary to measure the  $Z$ -parameters at the bias point of  $V_{ds}=0$ ,  $V_{gs}=-0.25$  V,  $0$  V,  $0.25$  V and  $0.5$  V, then plot the curve  $\text{Re}(Z_{ij})$  verse  $1/(V_{gs} - V_{th})$ . The intercept of  $\text{Re}(Z_{22})$  verse  $1/(V_{gs} - V_{th})$  is the extracted value of the sum of  $R_s$  and  $R_d$ , the intercept of  $\text{Re}(Z_{12})$  verse  $1/(V_{gs} - V_{th})$  is the extracted value of  $R_s$  as shown in Fig. 6 (a).

Similar to extracting resistances  $R_s$  and  $R_d$ , the resistance  $R_j$  is directly proportional to  $1/I_g$ <sup>[13]</sup>. Consequently, Eq. 21 can be expressed as:

$$\text{Re}(Z_{11}) \Big|_{1/I_g=0} = R_s + R_g \quad . \quad (26)$$

When the InP HEMT is biased at  $V_{ds}=0$  and different  $I_g$ , the resistance  $R_g$  can be calculated from Eq. 26. As shown in Fig. 6 (b), the intercept of  $\text{Im}(Z_{11})/(1/I_g)$  is the extracted value of the sum of  $R_s$  and  $R_g$ , then  $R_g$  can

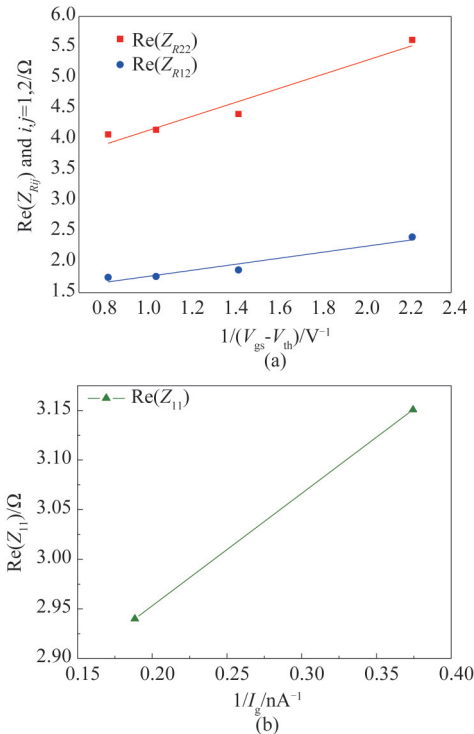


Fig. 6 Parasitic resistances extraction from the intercepts of (a)  $\text{Re}(Z_{ij})$  verse  $1/(V_{gs} - V_{th})$  and (b)  $\text{Re}(Z_{11})$  verse  $1/I_g$ . 图6 从(a)  $\text{Re}(Z_{ij})$  随  $1/(V_{gs} - V_{th})$  变化和(b)  $\text{Re}(Z_{11})$  随  $1/I_g$  变化的截距中提取寄生电阻

be obtained.

## 2.4 Extrinsic parameters verification

Before extracting intrinsic parameters, the accuracy of the extrinsic parameters needs to be verified. Complete extrinsic parameters of the pinch-off InP HEMT device ( $V_{ds}=0$ V,  $V_{gs}=-2$ V) small signal model are tabulated in Table 1.

Table 1 Extracted extrinsic parameters values for the small signal model of pinch-off InP HEMT  
表1 InP HEMT小信号模型夹断状态下的参数提取值

Extrinsic parameters	$V_{ds}=0$ V, $V_{gs}=-2$ V	Intrinsic parameters	$V_{ds}=0$ V, $V_{gs}=-2$ V
$R_g/\Omega$	1.353	$C_{gs}/\text{fF}$	70.000
$R_d/\Omega$	0.619	$C_{db}/\text{fF}$	52.958
$R_s/\Omega$	0.369	$C_{gd}/\text{fF}$	71.962
$L_g/\text{pH}$	33.405	$R_{is}/\Omega$	0
$L_d/\text{pH}$	25.569	$G_{ds}/\text{S}$	0.100
$L_j/\text{pH}$	8.256	$G_{gs}/\text{S}$	0
$C_{pg}/\text{fF}$	12.600	$G_m/\text{S}$	0
$C_{pd}/\text{fF}$	13.153	$\tau$ (ps)	0
$C_{pgd}/\text{fF}$	4.657		

## 3 Small signal model validation

After de-embedding the extrinsic parameters, the  $Y$  parameter can be used to determine the intrinsic parameters. Calculate the intrinsic parameters' values using Eqs. 27-33. Figures 7-10 show the extracted intrinsic parameters at  $V_{gs}=-0.75$ V,  $V_{ds}=4$ V.

$$C_{gs} = \frac{\text{Im}(Y_{11} - \omega C_{gd})}{\omega} \left( 1 + \frac{(\text{Re}(Y_{11}))^2}{(\text{Im}(Y_{11}) - \omega C_{gd})^2} \right), \quad (27)$$

$$R_{is} = \frac{\text{Re}(Y_{11})}{(\text{Im}(Y_{11}) - \omega C_{gd})^2 + (\text{Re}(Y_{11}))^2}, \quad (28)$$

$$C_{gd} = -\frac{\text{Im}(Y_{12})}{\omega}, \quad (29)$$

$$C_{ds} = \frac{\text{Im}(Y_{11}) - \omega C_{gd}}{\omega}, \quad (30)$$

$$G_{ds} = \text{Re}(Y_{22}) \quad , \quad (31)$$

$$g_m = \sqrt{[\text{Re}(Y_{21})^2 + (\text{Im}(Y_{21}) + \omega C_{gd})^2] \cdot (1 + \omega^2 C_{gs}^2 R_{is}^2)}, \quad (32)$$

$$\tau = \frac{1}{\omega} \arcsin \left[ \frac{-\omega C_{gd} - \text{Im}(Y_{21}) - \omega C_{gs} R_{is} \cdot \text{Re}(Y_{21})}{g_m} \right]. \quad (33)$$

It can be seen from Figs. 7-10 that the direct extraction method can obtain the average value of intrinsic parameters biased at  $V_{gs}=-0.75$ V,  $V_{ds}=4$ V, which can be optimized as the initial value of the numerical optimization method. Finally, the extrinsic and intrinsic parameters extracting with the proposed extraction method is shown in Table 2.

In order to verify the distributed small signal model of InP HEMT, the simulated results of the model need to be compared with the measured results. Figure 11 shows

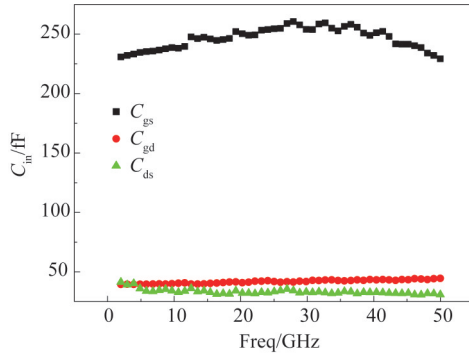


Fig. 7  $C_{in}$  values versus frequency  
图7  $C_{in}$ 随频率变化曲线

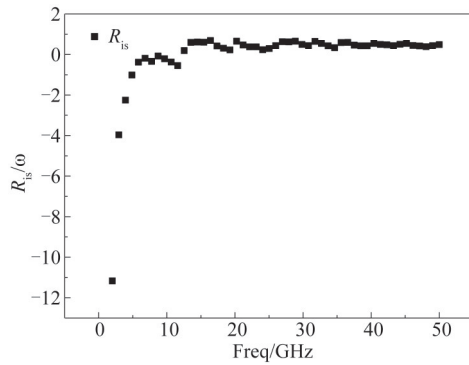


Fig. 8  $R_{is}$  values versus frequency  
图8  $R_{is}$ 随频率变化曲线

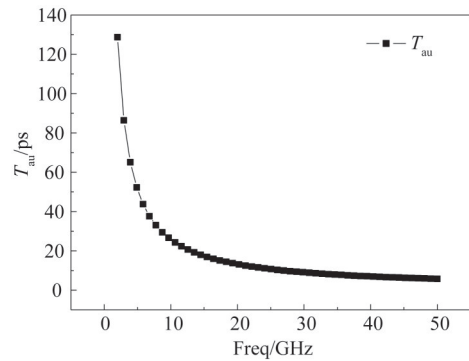


Fig. 9  $T_{au}$  values versus frequency  
图9  $T_{au}$ 随频率变化曲线

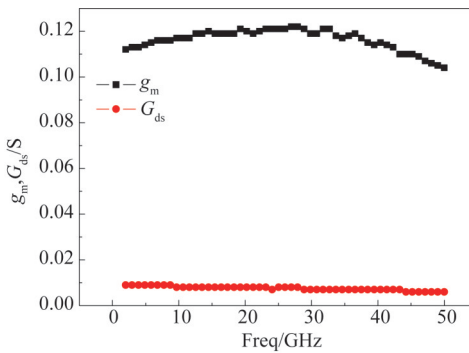


Fig. 10  $g_m, G_{ds}$  values versus frequency  
图10  $g_m, G_{ds}$ 随频率变化曲线

Table 2 Extracted parameters values for the small signal model of InP HEMT

表2 InP HEMT小信号模型的参数提取值

Extrinsic parameters	$V_{ds}=4\text{ V},$ $V_{gs}=-0.75\text{ V}$	Intrinsic parameters	$V_{ds}=4\text{ V},$ $V_{gs}=-0.75\text{ V}$
$R_g/\Omega$	1.353	$C_{gs}/\text{fF}$	217.800
$R_d/\Omega$	0.619	$C_{ds}/\text{fF}$	42.424
$R_s/\Omega$	0.369	$C_{gd}/\text{fF}$	47.839
$L_g/\text{pH}$	33.405	$R_{is}/\Omega$	0.286
$L_d/\text{pH}$	25.569	$G_{ds}/\text{S}$	0.008
$L_s/\text{pH}$	8.256	$G_{gs}/\text{S}$	0.021
$C_{pg}/\text{fF}$	12.600	$G_m/\text{S}$	0.112
$C_{pdf}/\text{fF}$	13.153	$\tau$ (ps)	0.830
$C_{pgd}/\text{fF}$	4.657		

the simulated S-parameters of the small-signal equivalent circuit of the InP HEMT including the distributed capacitances with the measured data. The comparison demonstrates good agreement from 2 ~ 50 GHz, which also verifies the validity of the model and extraction method.

To further evaluate the accuracy of the small signal model, the modeling error is defined as:

$$\text{Error} = \sum_{ij=1,2} \frac{|S_{s,ij} - S_{m,ij}|}{0.5 \times |S_{s,ij} + S_{m,ij}|} \sqrt{4}, \quad (34)$$

where  $S_{s,ij}$  is the simulated data and  $S_{m,ij}$  is the measured data. As shown in Fig. 12, it is obvious that the modeling error is less than 4% in the frequency range of 2~50 GHz, which mathematically proves the accuracy of the small signal model.

## 4 Conclusion

A distributed small signal extraction method for  $4 \times 75 \mu\text{m}$  gate width,  $0.15 \mu\text{m}$  gate length InP HEMT is proposed in this paper. Before extracting the parasitic capacitance, the parasitic inductances are first de-embedded to eliminate errors. The extrinsic capacitances including distributed and parasitic capacitances are determined at four different gate widths using algorithmic optimization and a gate-width scalable method. The values of the model parameters obtained by the direct extraction method are used as the initial values of the optimization method for model optimization. Finally, there is good agreement between the measured and simulated S-parameters up to 50 GHz.

## References

- [1] Kulatunga T, Belostotski L, and Haslett J W. 400-to-800-MHz GaAs pHEMT-Based wideband LNA for radio-astronomy antenna-array feed [J]. *IEEE Microwave and Wireless Components Letters*, 2018, **28** (10):99-911.
- [2] GAO Jian-Jun. *RF and microwave modeling and measurement techniques for field effect transistors* [M]. Raleigh, NC: SciTech Publishing, 2010.
- [3] Dambrine G, Cappy A, Heliodore F. A new method for determining the FET small-signal equivalent circuit [J]. *IEEE Transactions on microwave theory and techniques*, 1988, **36**(7): 1151-1159.
- [4] Berroth M, Bosch R. High-frequency equivalent circuit of InP FETs for large-signal applications [J]. *IEEE transactions on Microwave*

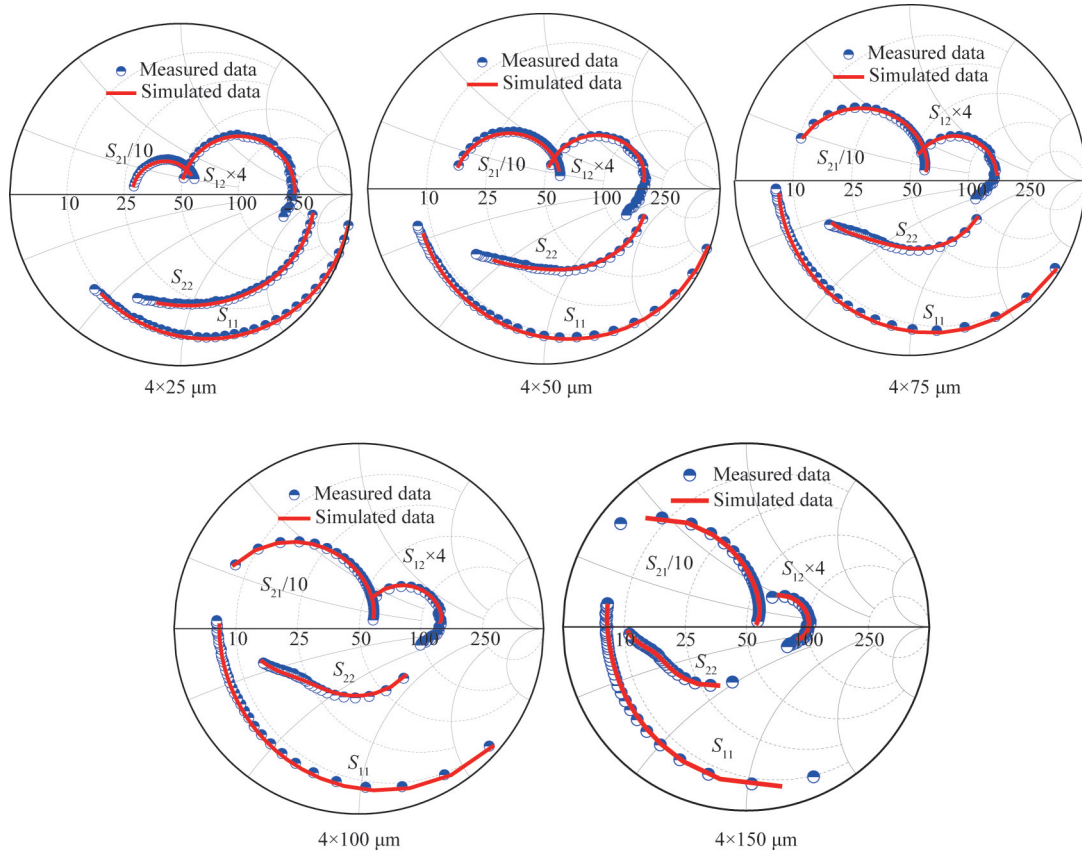


Fig. 11 Simulated and measured results of InP HEMT biased at  $V_{ds}=4\text{ V}$ ,  $V_{gs}=-0.75\text{ V}$   
 图 11 InP HEMT 在偏置为  $V_{ds}=4\text{ V}$ ,  $V_{gs}=-0.75\text{ V}$  时的仿真结果和测试结果

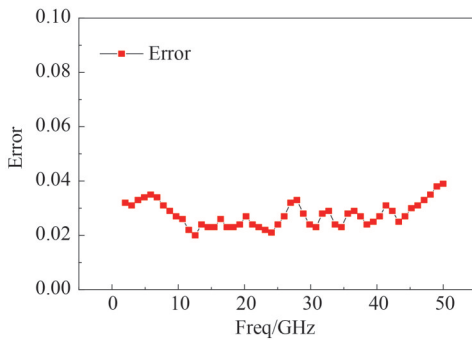


Fig. 12 S-parameter modeling error of InP HEMT small signal model  
 图 12 InP HEMT 小信号模型的 S 参数建模误差

*Theory and Techniques*, 1991, **39**(2): 224–229.

- [5] Jarndal A, Kompa G. A new small signal model parameter extraction method applied to GaN devices [C]. *IEEE MTT-S International Microwave Symposium Digest*, 2005, Oct. pp: 1423–1426.  
 [6] Fan C.Y., Gao J.J. A semi-analytical small signal parameter extrac-

tion method for millimeter HEMT [J]. *J. Infrared Millim. Waves*, 2014, **33**(1): 69–74.

- [7] ZHANG Jin-Can, WANG Shao-Wei, LIU Min, *et al.* An improved GaN P-HEMT small-signal equivalent circuit with its parameter extraction [J]. *Microelectronics journal*, 2021, **112**(1): 105042.  
 [8] Nguyen T T L, Kim S D. A gate-width scalable method of parasitic parameter determination for distributed HEMT small-signal equivalent circuit [J]. *IEEE Transactions on Microwave Theory and Techniques*, 2013, **61**(10): 3632–3638.  
 [9] Gao J, Li X, Wang H. A new method for determination of parasitic capacitances for HEMT [J]. *Semiconductor science and technology*, 2005, **20**(6): 586.  
 [10] Jarndal A, Kompa G. A new small-signal modeling approach applied to GaN devices [J]. *IEEE Transactions on Microwave Theory and Techniques*, 2005, **53**(11): 3440–3448.  
 [11] Hower P L, Bechtel N G. Current saturation and small-signal characteristics of InP field-effect transistors [J]. *IEEE Transactions on Electron Devices*, 1973, **20**(3): 213–220.  
 [12] Berroth M, Bosch R. Broad-band determination of the FET small-signal equivalent circuit [J]. *IEEE Transactions on Microwave Theory and techniques*, 1990, **38**(7): 891–895.  
 [13] Alt A R, Marti D, and Bolognesi C R. Transistor modeling: Robust small-signal equivalent circuit extraction in various HEMT technologies [J]. *IEEE Microwave Magazine*, 2013, **14**(4): 83–101.